

*Supplementary Information for*

**Trace level detection of nitroanilines by a solution processable fluorescent porous organic polymer**

**Arundhati Deshmukh, Sujoy Bandyopadhyay, Anto James and Abhijit Patra\***

Department of Chemistry, Indian Institute of Science, Education and Research (IISER)

Bhopal, Bhopal-462066, Fax: +91 (0)755 409 2392; Tel: +91 (0)755 669 2378

E-mail: abhijit@iiserb.ac.in

**CONTENTS**

<b>I. Experimental Section</b>	2-5
(a) Materials	
(b) Characterizations of TPDC-DB polymer ( <sup>1</sup> H-NMR, FTIR, FESEM, TGA, PXRD)	
(c) Surface area of TPDC-DB polymer	
<b>II. Structure of analytes</b>	6
<b>III. Details of absorption and fluorescence spectroscopy</b>	7-16
(a) Spectroscopy of TPDC-DB	
(b) Quenching efficiency	
(c) Fluorescence titration	
(d) Fluorescence decays of TPDC-DB	
(e) Absorption-emission overlap	
(f) Effect of temperature on quenching	
<b>IV. DFT calculations</b>	17
<b>V. Electron paramagnetic resonance (EPR) spectroscopy</b>	18
<b>VI. Fitting curves for Stern-Volmer plots</b>	19
<b>VII. Interactions of PNA and PA with TPDC-DB</b>	20-21
<b>VIII. Limit of detection</b>	
(a) Solution	22
(b) Contact Mode	23
<b>IX. Detection of PNA in presence of competing analytes</b>	23
<b>X. Solid-state contact mode detection</b>	24
<b>XI. Comparison of TPDC-DB with reported nitroaniline sensors</b>	25
<b>XII. References</b>	26

## I. Experimental Section

**(a) Materials:** *p*-nitroaniline (PNA, 99%), *o*-nitroaniline (ONA, 98%), *m*-nitroaniline (MNA, 98%), 2,4-dinitroaniline (DNA, 98%), 2,6-dichloro-*p*-nitroaniline (DCPNA, 96%), *o*-nitrophenol (ONP, 98%), *p*-nitrophenol (PNP, 99%), 9,10-phenanthraquinone (PAQ, 98%), 1-chloroanthraquinone (CIAQ, 98%), 2,4-dinitrobenzaldehyde (DNB, 97%), nitrobenzene (NB, 99%), *p*-nitrobenzaldehyde (PNB, 99%), 2,4-dinitrotoluene (DNT, 97%), *p*-nitrotoluene (PNT, 99%), mesitylene (Mes, 97%), *p*-nitrobenzoic acid (PNBA, 98%), 1,2-dichlorobenzene (DCB, 98%), acrylamide (Acry, 98%), trifluoroacetic acid (TFA, 98%), *p*-benzoquinone (PBQ, 97%), aniline (99.5%), phenol (99%), nitromethane (NM, 99%), chlorobenzene (BCl, 99%) and 1,4-dibromobenzene (DBB, 98%), 1,4-diethynylbenzene (DB, 95%), bis(triphenylphosphine)palladium(II)dichloride (98%), diisopropylamine (DIPA, 99%), trimethylamine (TEA, 99.5%), *n*-octylamine (NOA, 99%) were obtained from Sigma-Aldrich. Picric acid (PA, 99%) was obtained from Merck and 2,3-dichloro-5,6-dicyano-1,4-benzoquinone (DDQ, 99%) was obtained from Alfa Aesar. PNA, DNA and PA were recrystallized from ethanol and all the other analytes were used as received. Coumarin-102 in ethanol was used as a standard for quantum yield measurements. All the solutions were made in spectroscopic grade THF obtained from Spectrochem. Non-fluorescent TLC plates for solid state contact mode detection were obtained from Merck.

### **(b) Characterizations of TPDC-DB polymer:**

GPC (THF):  $M_n = 13$  kDa,  $M_w = 16$  kDa;  $^1\text{H NMR}$  (700 MHz;  $\text{CDCl}_3$ , 23°C, TMS):  $\delta = 7.50 - 7.47$  (m, Ar-H), 7.43 – 7.31 (m, Ar-H), 7.20 (br, Ar-H), 7.01 (br, Ar-H), 6.90 (br, Ar-H), 6.77 (br, Ar-H), 6.66 (br, Ar-H), 1.71 (m,  $\text{CH}_2$ ), 1.34 – 1.07 (br,  $\text{CH}_2$ ), 0.86 ppm (t,  $\text{CH}_3$ ); FTIR:  $\nu$  bar = 3035, 2925, 2850, 2205, 1595, 1485, 830  $\text{cm}^{-1}$ ; EDX analysis (wt%): C 98.51, Br 1.07, Pd 0.42.

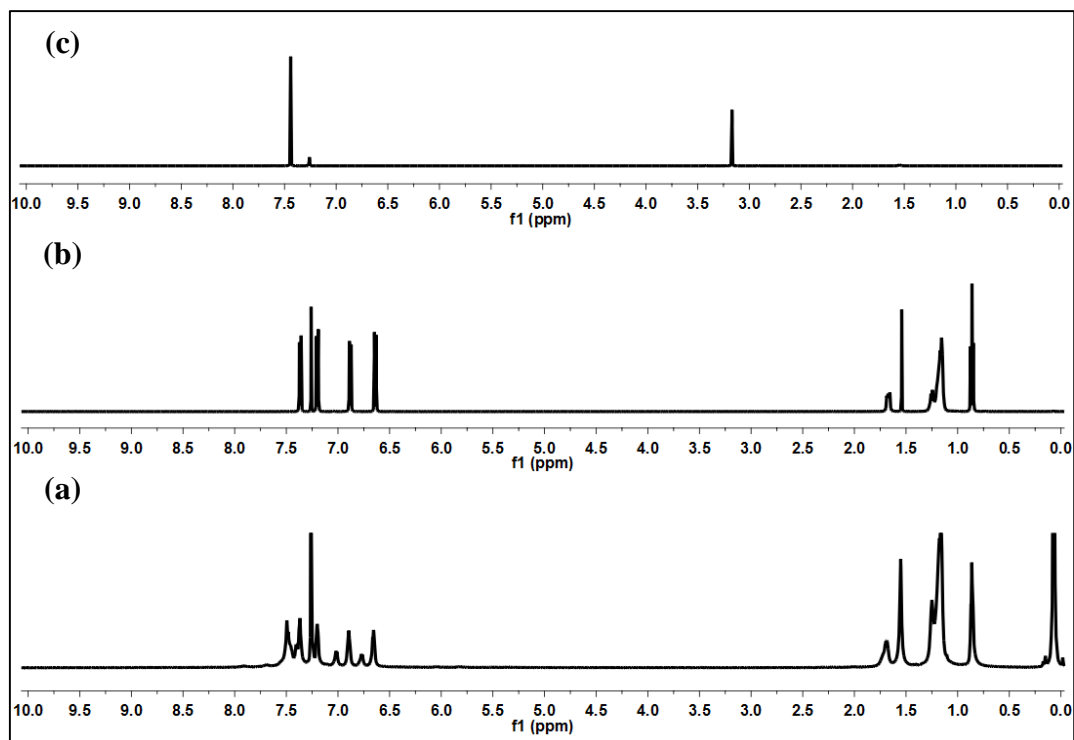


**Fig. S1.**  $^1\text{H}$  NMR spectra of (a) TPDC-DB, (b) TBDC and (c) DB.

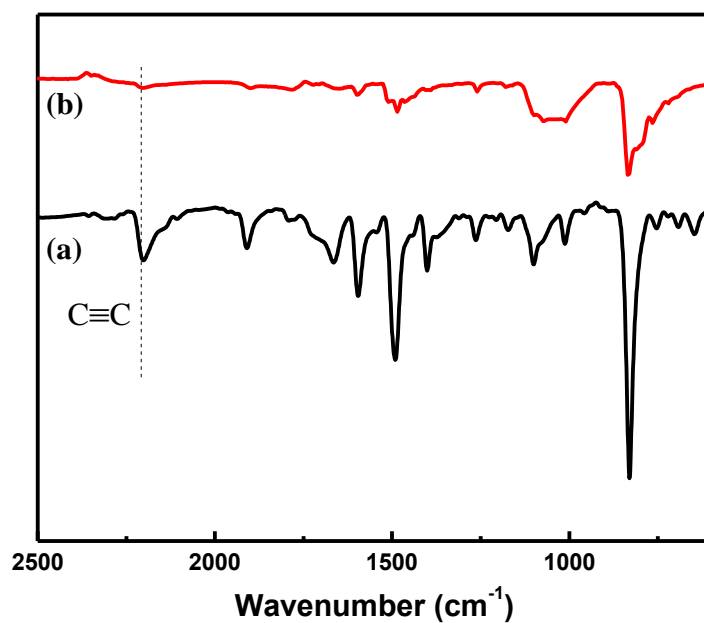


**Fig. S2.** FTIR spectra of TPDC-DB: (a) insoluble solid and (b) solution processable form.

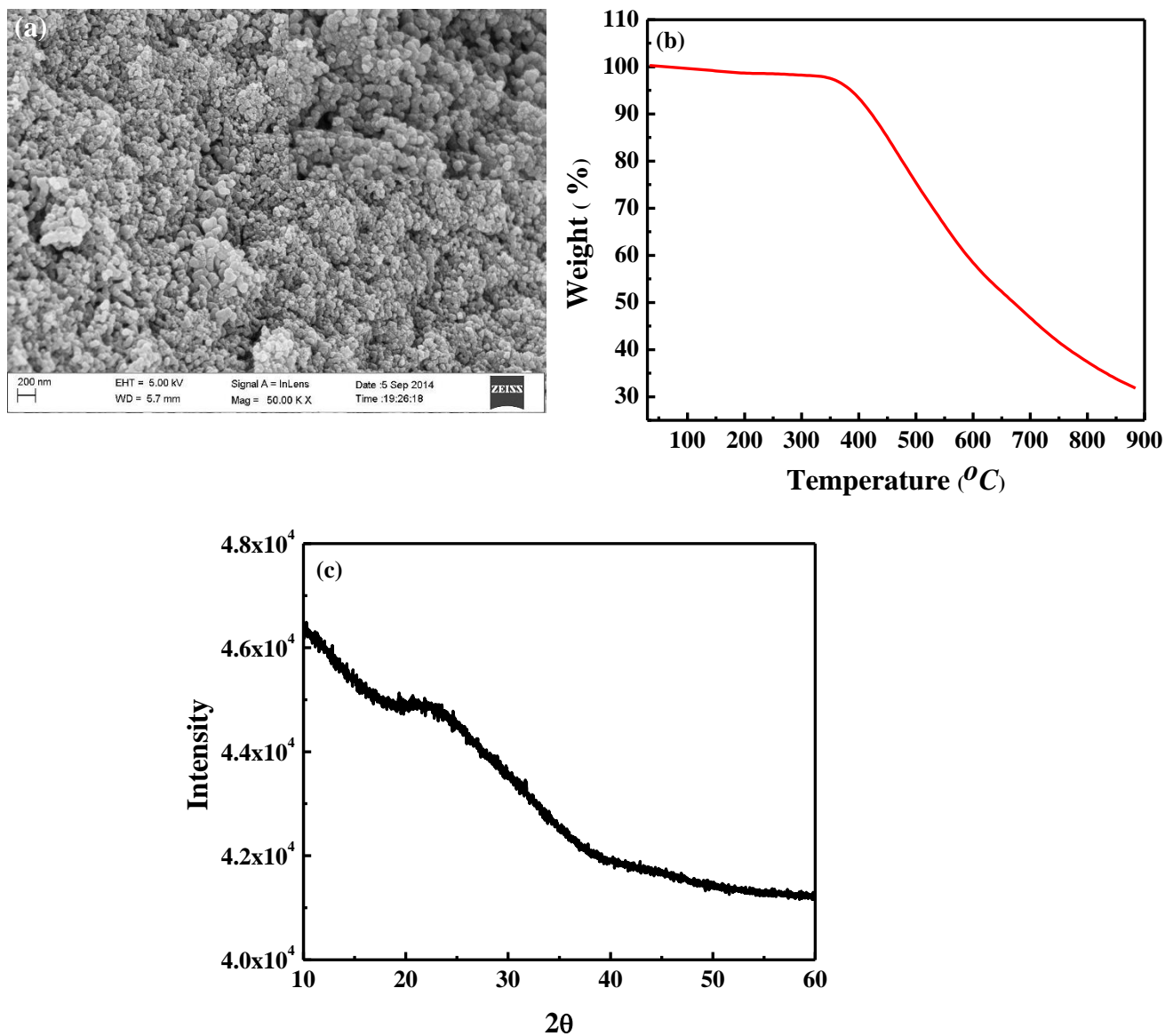


**Fig. S3.** Characterizations of solution processable TPDC-DB polymer obtained in the form of powder after precipitation and subsequent drying: (a) Field Emission Scanning Electron Micrograph (FESEM) image (top right: magnified view), (b) Thermogravimetric analysis (TGA) and (c) powder X-ray diffraction (PXRD) pattern.

**(c) Surface area of TPDC-DB polymer:** BET surface area of TPDC-DB polymer was found to be  $39 \text{ m}^2\text{g}^{-1}$ , estimated from  $\text{N}_2$  gas adsorption experiments performed on a Quantachrome Autosorb QUA211011 equipment at 77 K. Total pore volume was estimated to be  $0.26 \text{ cm}^3\text{g}^{-1}$ . Pore size distribution (Fig. S4, inset) calculated by nonlocal density function theory (NLDFT) method revealed that the pores are centered mostly at 3.1 nm.

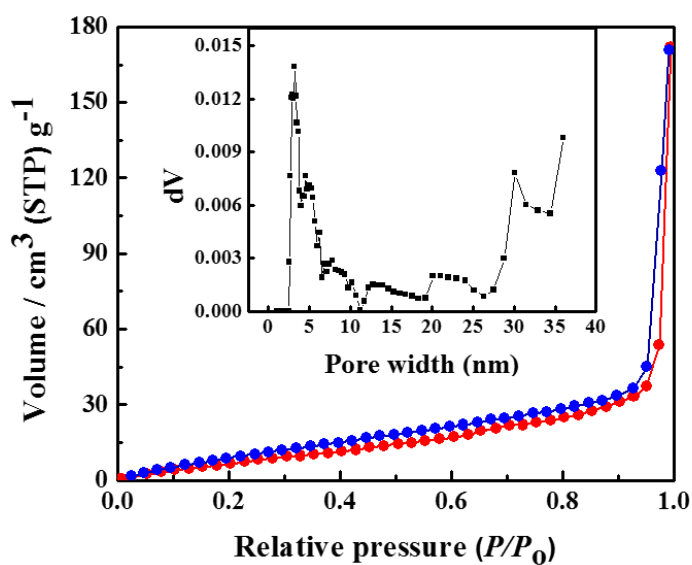


**Fig. S4.** Nitrogen sorption isotherms (red: adsorption; blue: desorption) of TPDC-DB measured at 77 K. Inset: pore-size distribution profile estimated using the NLDFT method.

## II. Molecular structure of analytes investigated

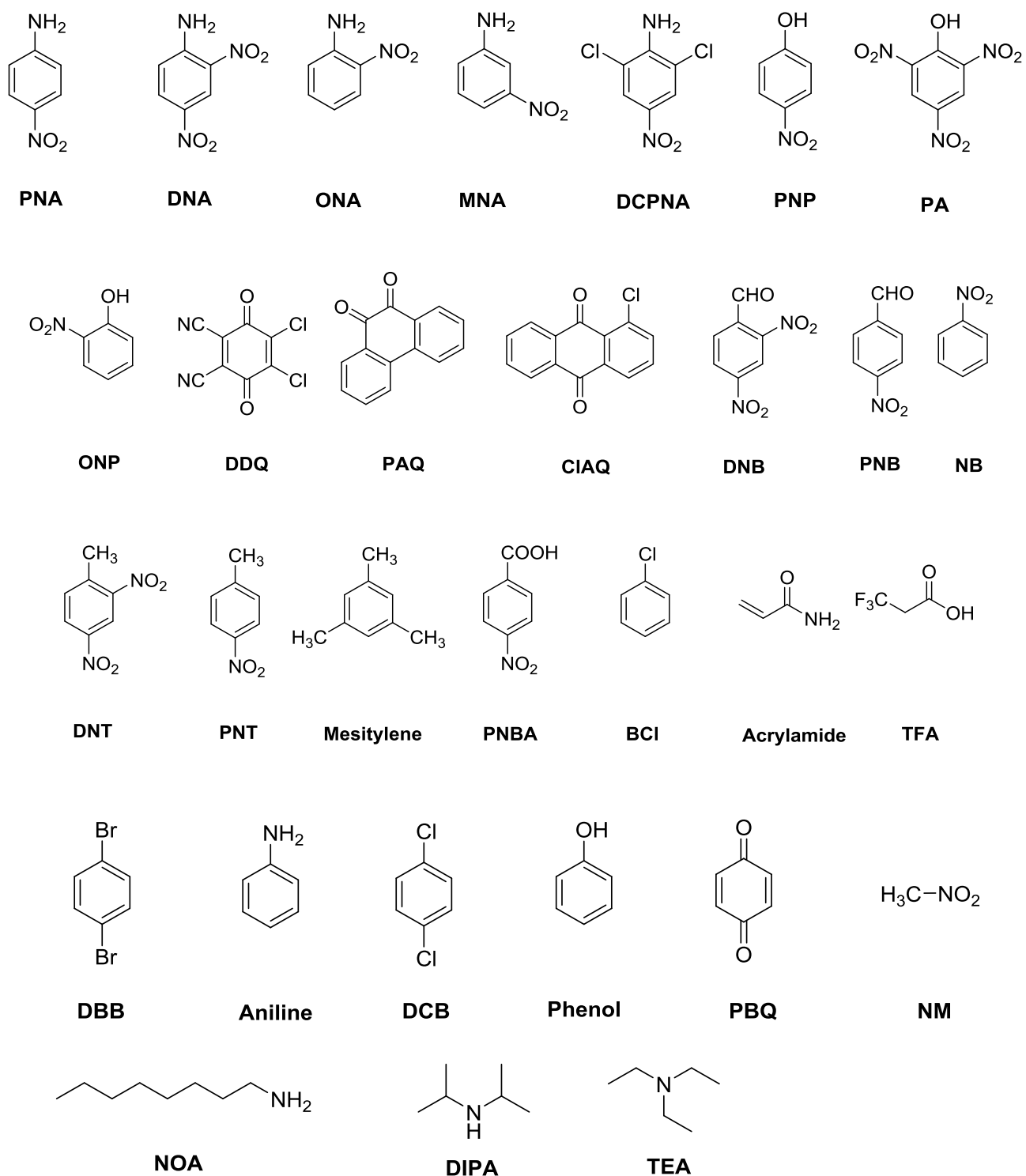
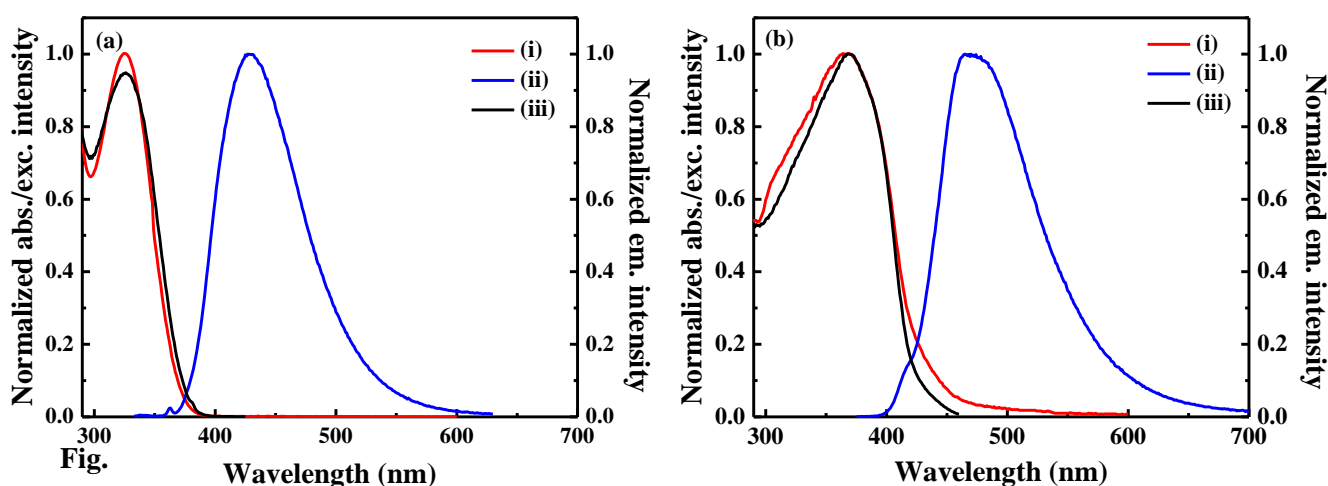


Chart S1. Molecular structures of 30 analytes investigated for the quenching study.

### III. Details of absorption and fluorescence spectroscopy

**(a) Spectroscopy of TPDC-DB:** Normalized absorption, emission and excitation spectra of a THF solution of TPDC-DB and the monomer TPDC are shown in Fig. S5. Absorption maxima of TPDC-DB is obtained at  $\lambda = 365$  nm significantly red shifted from that of TPDC ( $\lambda = 325$  nm), indicating extended conjugation in TPDC-DB. The absorption band can be assigned to  $\pi-\pi^*$  transition of the conjugated network. Emission maxima for TPDC-DB and TPDC respectively are at  $\lambda = 468$  nm and  $\lambda = 430$  nm. Excitation spectra of both monomer and polymer are matching with their respective absorption spectra indicating that emission is arising from the same state to which direct absorption occurs. The spectroscopic data is compiled in Table S1.



**Fig. S5.** Normalized (i) absorption (ii) emission and (iii) excitation spectra of a THF solution of (a) monomer TPDC and (b) TPDC-DB polymer.

**Fluorescence quantum yield ( $\phi_f$ ) measurement:** The fluorescence quantum yields of TPDC-DB and monomer TPDC in THF were estimated by comparison with Coumarin-102 in ethanol ( $\Phi_f = 0.76$ ).<sup>1</sup> The quantum yields were calculated using the following equation.<sup>2</sup>

$$\Phi_{f,x} = \Phi_{f,s} \cdot \frac{F_x}{F_s} \cdot \frac{f_s}{f_x} \cdot \frac{n_x^2}{n_s^2}$$

where,  $\Phi_f$  is fluorescence quantum yield, subscript x denotes unknown sample and subscript s refers to standard. F denotes integral fluorescence, n refers to refractive index of the solvent used in the measurements and f is the absorption factor at the excitation wavelength given by the following equation:

$f = 1 - 10^{-\varepsilon(\lambda_{ex})cl} = 1 - 10^{-A(\lambda_{ex})}$ , where A is absorbance and  $\varepsilon$  = molar extinction coefficient in  $L \text{ mol}^{-1} \text{ cm}^{-1}$ .

**Table S1:** A comparative table of spectroscopic properties of TPDC and TPDC-DB in THF solution.

Compound name	$\lambda_{\text{abs}}$ (nm)	$\lambda_{\text{ex}}$ (nm)	$\lambda_{\text{em}}$ (nm)	Quantum yield
TPDC	325 nm	325 nm	430 nm	7 %
TPDC-DB	365 nm	365 nm	468 nm	27 %

**(b) Quenching efficiency:** Relative quenching efficiencies (QE) for all the 30 analytes are shown in Fig. S6. QE of each analyte was calculated after inner-filter effect (IFE) correction (following eqn 2 in the main text). As shown in Fig. S6, a strong acid such as TFA shows no quenching implying acidity is not a governing factor. Moreover, a small increase in the fluorescence intensity (3-5%) was obtained for electron-rich analytes such as BCl and DBB (Chart S1).

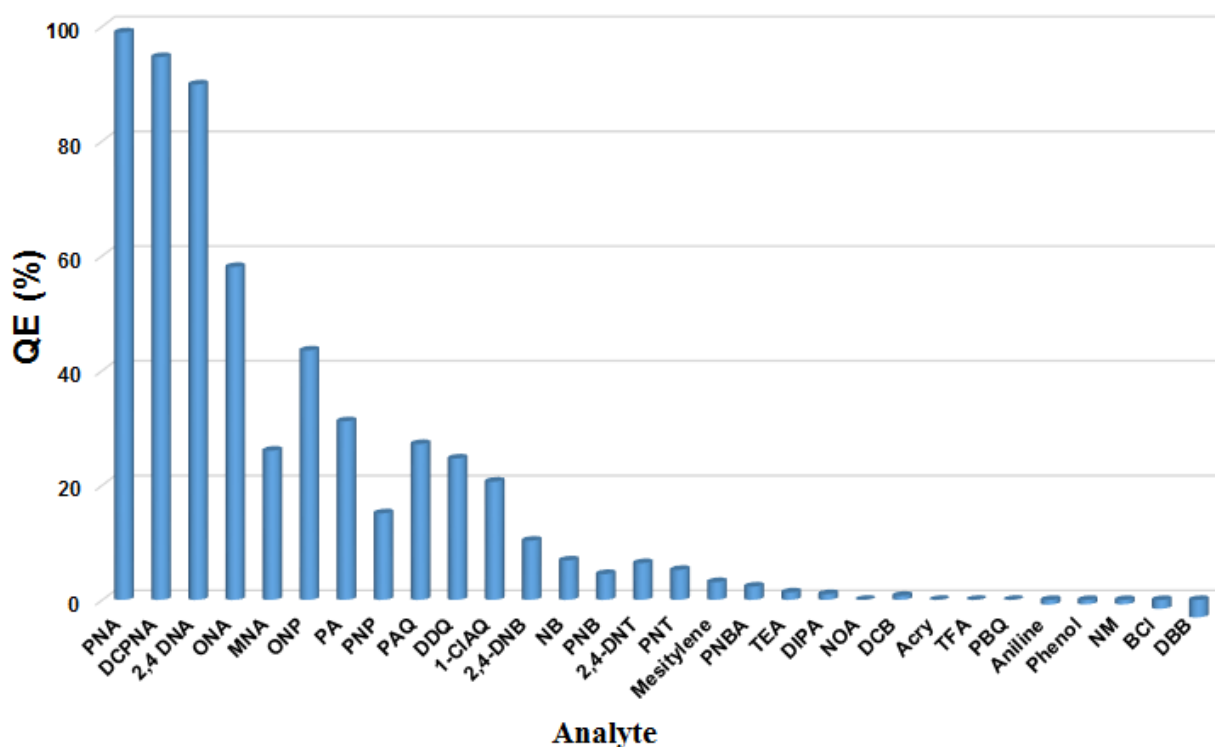


**Fig. S6.** Percentage quenching efficiency after addition of 10  $\mu\text{L}$ , 0.1 M solution of each analyte to a solution of TPDC-DB polymer with fixed concentration.

**(c) Fluorescence titration:** For fluorescence titration experiments, 10 mM stock solutions of *p*-nitroaniline (PNA), 2,6-dichloro-4-nitroaniline (DCPNA) and 2,4-dinitroaniline (DNA) and 40 mM solution of *o*-nitroaniline (ONA) were prepared. To a 0.02 mg mL<sup>-1</sup> solution of TPDC-DB, the analytes were added in gradual intervals until ~99 % quenching was obtained.

Absorption, emission spectra and lifetime were taken at each interval. Fluorescence intensities were corrected for IFE. Fluorescence titration curves and Stern-Volmer plots for PNA, DCPNA, DNA and ONA are shown in the main text (Fig. 2); those for ONP, MNA, PA and DDQ are shown in Fig. S7-S10 respectively.

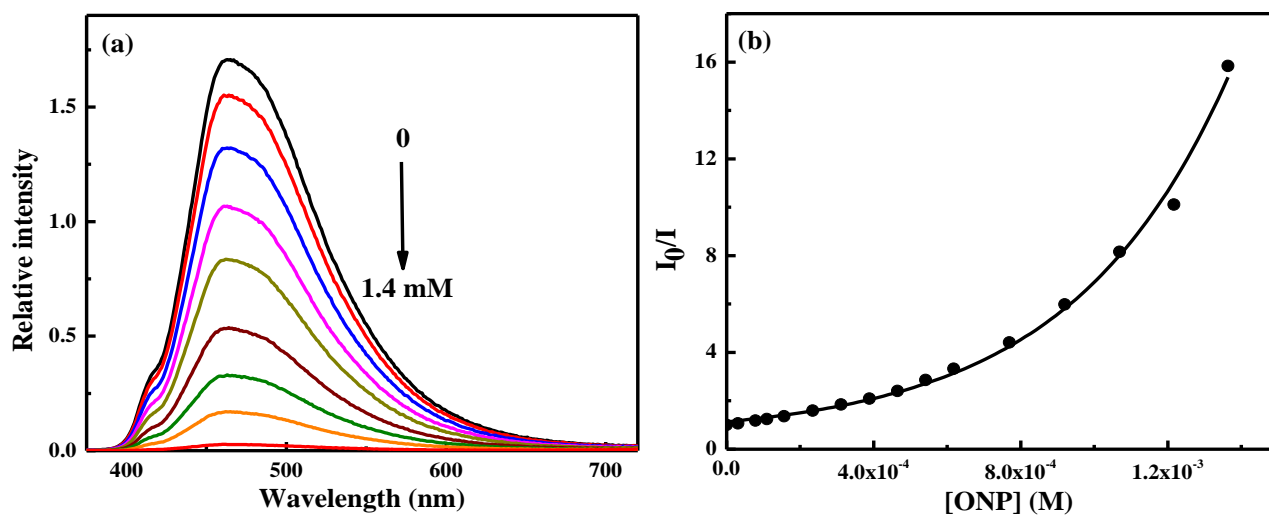


**Fig. S7.** (a) Emission spectra demonstrating the fluorescence quenching of TPDC-DB in THF ( $\lambda_{\text{ex}} = 365$  nm) with increasing concentrations of ONP. (b) Stern-Volmer plot of  $I_0/I$  against the concentration of ONP.

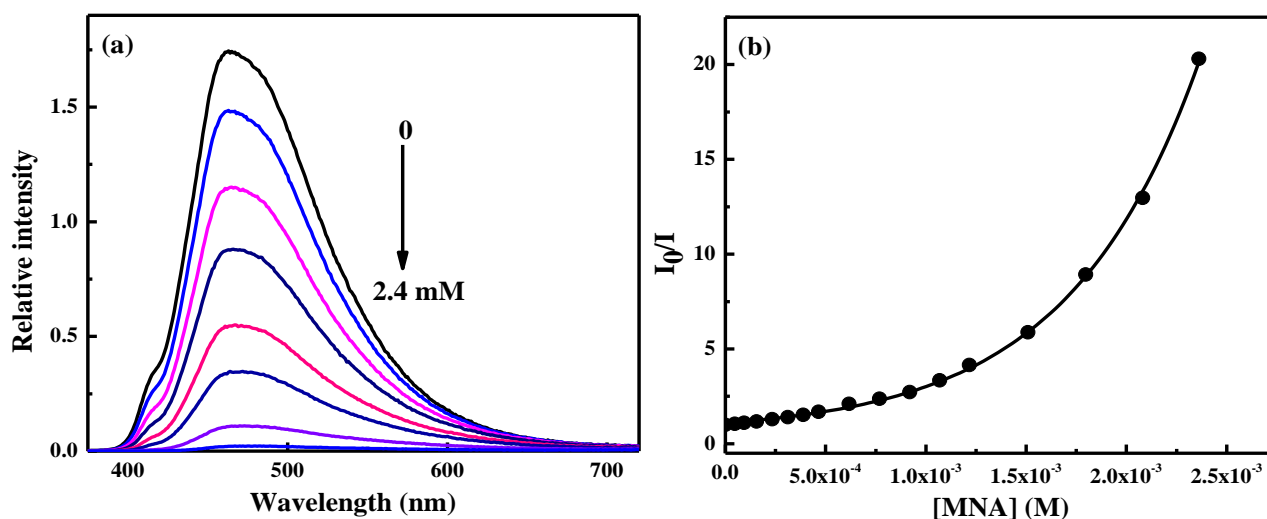


**Fig. S8.** (a) Emission spectra demonstrating the fluorescence quenching of TPDC-DB in THF ( $\lambda_{\text{ex}} = 365$  nm) with increasing concentrations of MNA. (b) Stern-Volmer plot of  $I_0/I$  against the concentration of MNA.

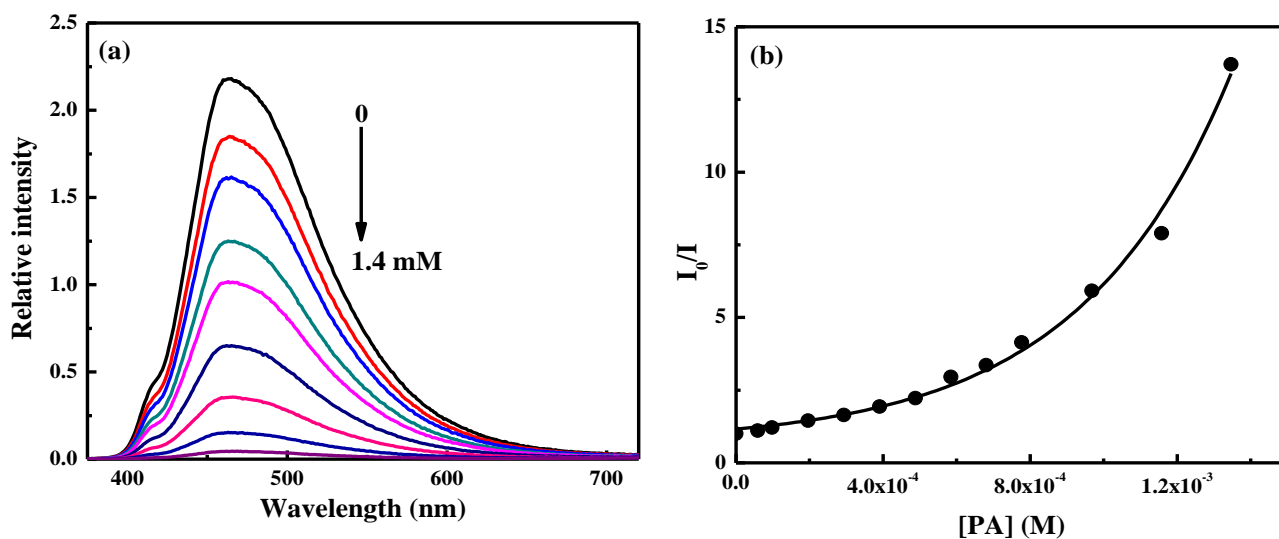


**Fig. S9.** (a) Emission spectra demonstrating the fluorescence quenching of TPDC-DB in THF ( $\lambda_{\text{ex}} = 365$  nm) with increasing concentrations of PA. (b) Stern-Volmer plot of  $I_0/I$  against the concentration of PA.

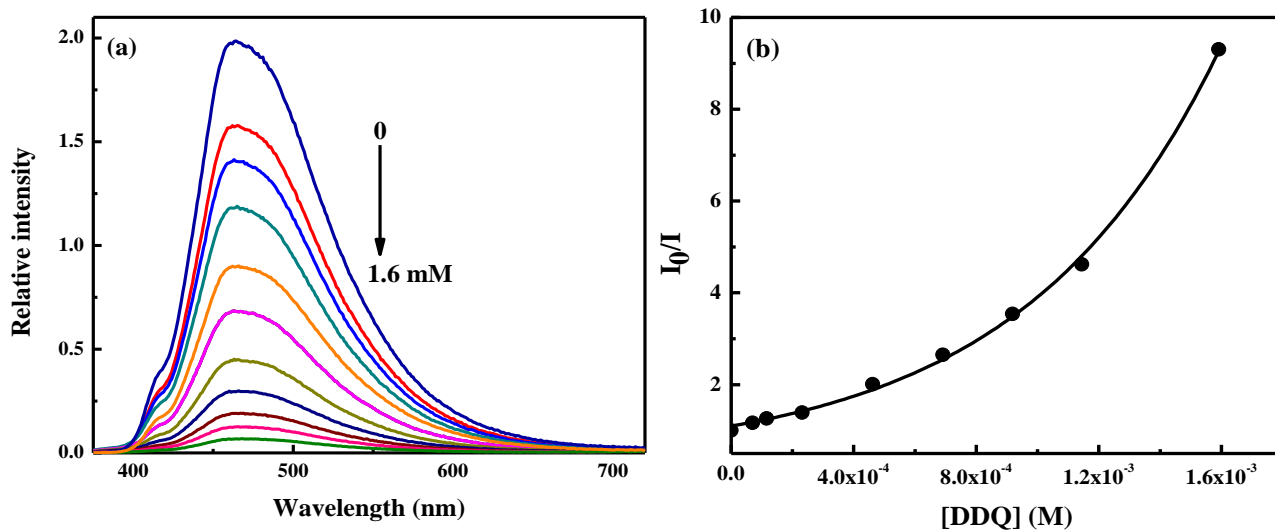


**Fig. S10.** (a) Emission spectra demonstrating the fluorescence quenching of TPDC-DB in THF ( $\lambda_{\text{ex}} = 365$  nm) with increasing concentrations of DDQ. (b) Stern-Volmer plot of  $I_0/I$  against the concentration of DDQ.

**(d) Fluorescence decays of TPDC-DB:** Fluorescence decay profile of TPDC-DB is shown in Fig. S11. Black continuous line represents the fit to the decay curve. Lifetime of pure TPDC-DB follows a bi-exponential decay. The average lifetime of TPDC-DB is 0.9 ns.

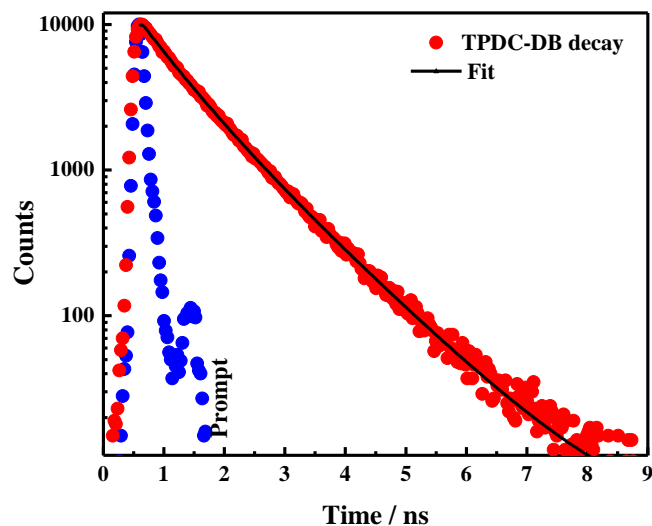


**Fig. S11.** Fluorescence decay profile ( $\lambda_{\text{ex}} = 370$  nm,  $\lambda_{\text{em}} = 468$  nm) of TPDC-DB in THF solution. Continuous black line indicates fit to the decay curve.

Decay profiles of TPDC-DB before and after almost complete quenching by the analytes are shown in the following Fig. S12-S15. The decay profiles perfectly overlap each other indicating no change in the lifetime upon the addition of quenchers. This is also evident from Table S2 where individual decay components, average lifetimes and  $\chi^2$  values are shown for gradual addition of PNA.

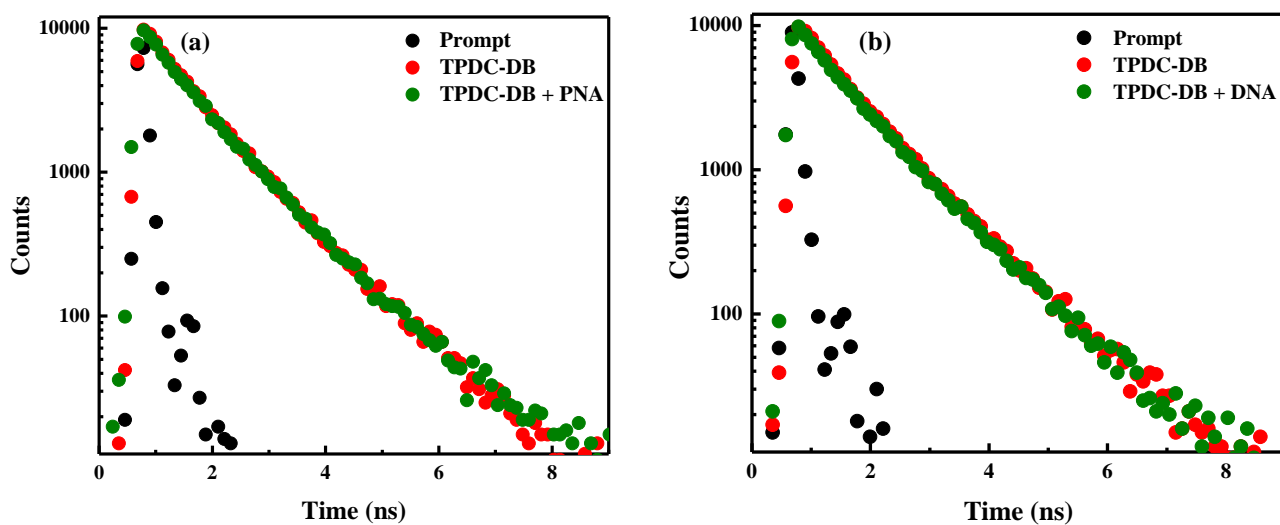


**Fig. S12.** Fluorescence decay profiles of TPDC-DB ( $\lambda_{\text{ex}} = 370$  nm,  $\lambda_{\text{em}} = 468$  nm) before (red) and after (green) addition of (a) PNA and (b) DNA.

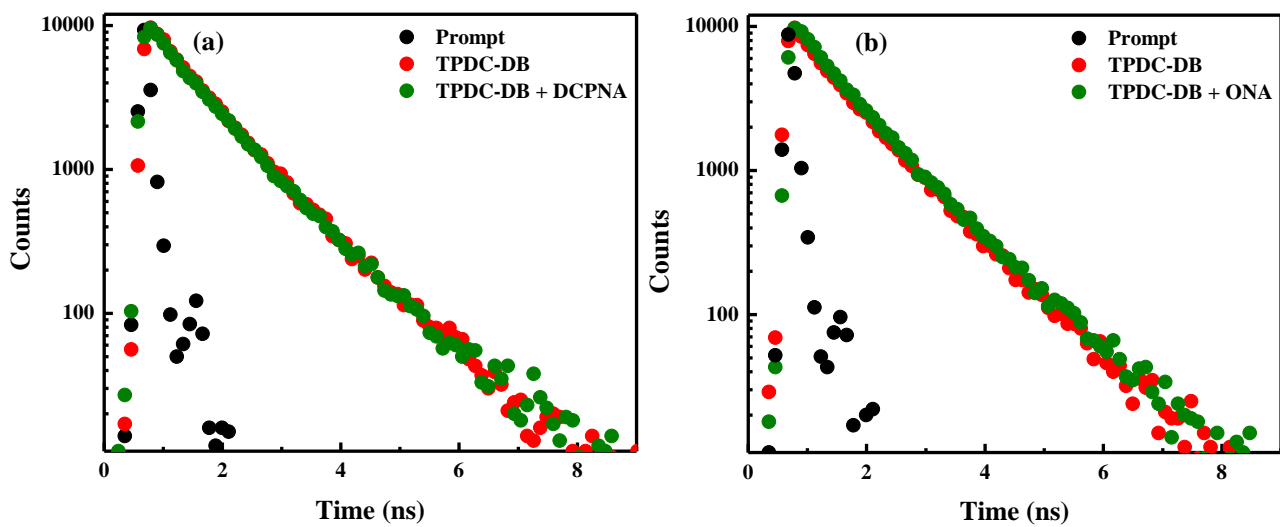


**Fig. S13.** Fluorescence decay profiles of TPDC-DB ( $\lambda_{\text{ex}} = 370$  nm,  $\lambda_{\text{em}} = 468$  nm) before (red) and after (green) addition of (a) DCPNA and (b) ONA.

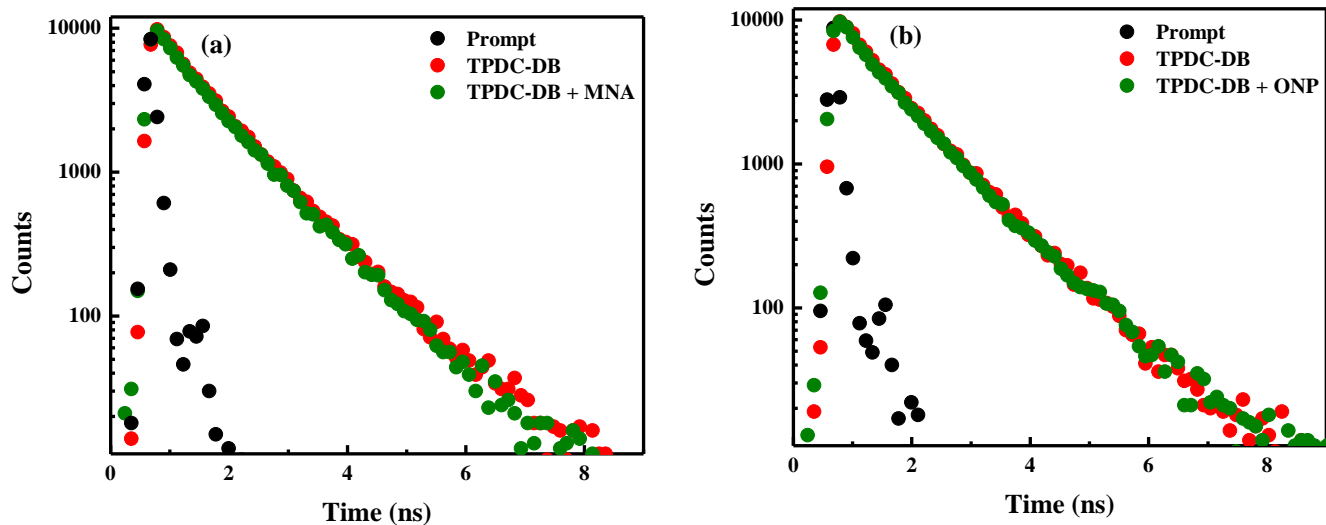


**Fig. S14.** Fluorescence decay profiles of TPDC-DB ( $\lambda_{\text{ex}} = 370$  nm,  $\lambda_{\text{em}} = 468$  nm) before (red) and after (green) addition of (a) MNA and (b) ONP.

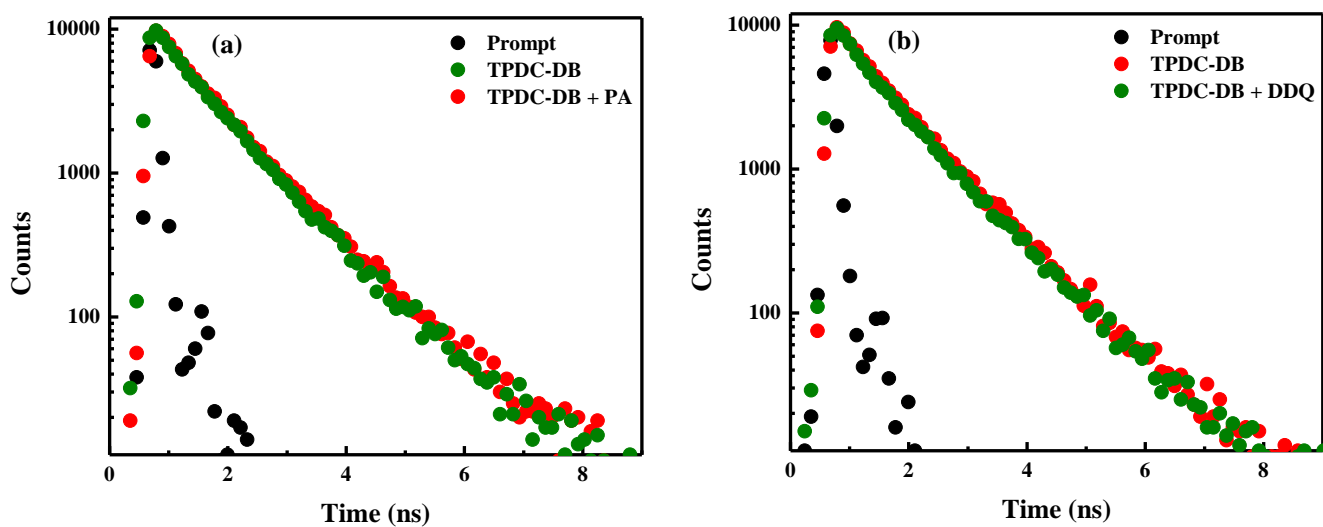


**Fig. S15.** Fluorescence decay profiles of TPDC-DB ( $\lambda_{\text{ex}} = 370$  nm,  $\lambda_{\text{em}} = 468$  nm) before (red) and after (green) addition of (a) PA and (b) DDQ.

**Table S2.** Fluorescence decay parameters for TPDC-DB in THF upon successive addition of PNA; the lifetimes ( $\tau_1$  and  $\tau_2$ ) and the respective fractional contributions ( $\alpha_1$  and  $\alpha_2$ ), the weighted average lifetime ( $\tau_{avg}$ ) and the quality of fitting ( $\chi^2$ ).

[PNA] ( $\times 10^{-4}$ M)	$\tau_1$ (ns)	$\alpha_1$	$\tau_2$ (ns)	$\alpha_2$	$\tau_{avg}$ (ns)	$\chi^2$
0	0.68	53	1.19	47	0.92	1.05
0.16	0.63	42	1.16	58	0.93	1.08
0.39	0.60	38	1.13	62	0.93	1.11
0.58	0.55	36	1.18	64	0.95	1.03
0.78	0.63	39	1.14	61	0.94	0.94
0.97	0.72	49	1.20	51	0.96	0.98
1.16	0.59	38	1.12	62	0.92	1.11
1.35	0.65	51	1.18	49	0.91	1.00
1.54	0.71	56	1.29	44	0.96	1.05
1.73	0.59	42	1.17	58	0.92	1.14
1.92	0.60	38	1.13	62	0.95	1.11
2.11	0.63	39	1.14	61	0.94	1.07
2.30	0.67	51	1.19	49	0.92	1.09
2.67	0.63	39	1.14	61	0.94	1.08

**(e) Absorption-emission overlap:** As shown in Fig. S16 (a-d), no significant spectral overlaps of ONP, MNA, PA and DDQ absorption and TPDC-DB emission are observed; similar trends were obtained for other analytes discussed in Fig. 3 in the main text.

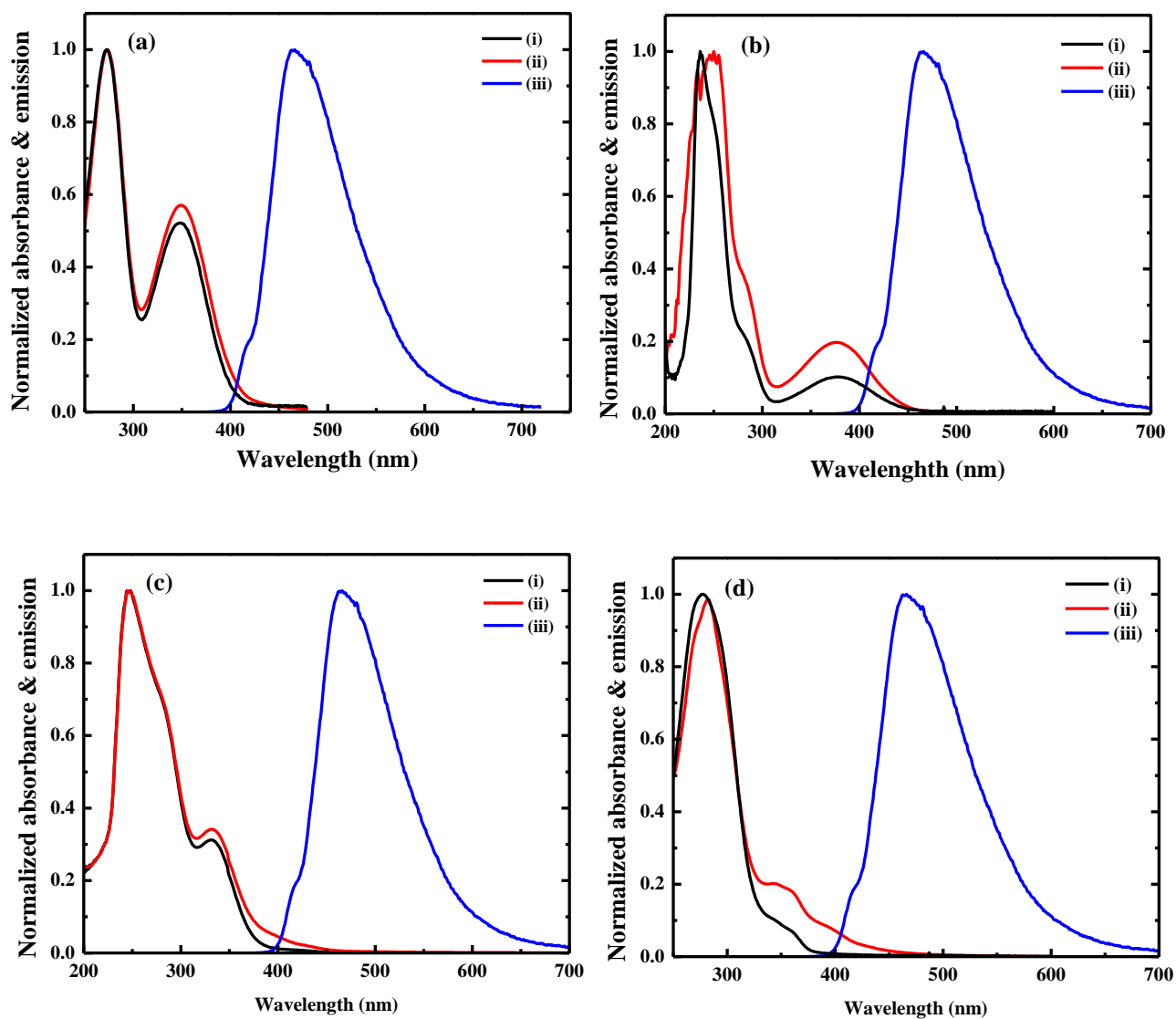


**Fig. S16.** (i) Normalized absorption spectra of (a) ONP, (b) MNA, (c) PA and (d) DDQ; (ii) normalized absorption spectra of a mixture of TPDC-DB with the corresponding analyte and (iii) normalized emission spectrum of TPDC-DB.

**(f) Effect of temperature on quenching:** Quenching of TPDC-DB by PNA was studied at various temperatures ranging from 298 to 318 K; corresponding Stern-Volmer plots are depicted in Fig. S17. No general trend (steady increase/decrease) can be seen in the slopes of Stern-Volmer plots. This observation further confirms no likelihood of a dynamic component or a ground-state complex.

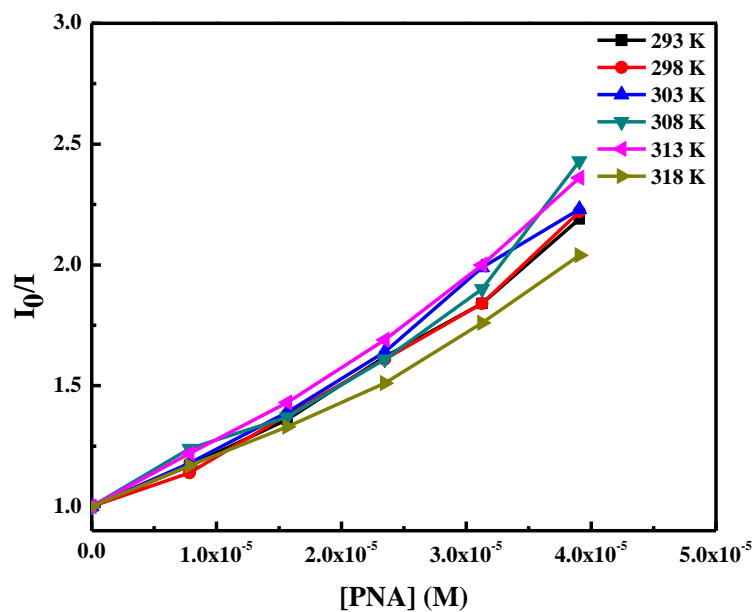


**Fig. S17.** Stern-Volmer plots of TPDC-DB quenching by PNA at 293, 298, 303, 308, 313 and 318 K.

#### IV. DFT calculations

HOMO and LUMO energy values for the first generation structure of TPDC-DB, (TPDC-DB)<sub>1</sub> and analytes were calculated using density functional theory (DFT) with Gaussian 09 software employing 6-31G(d) basis set and the B3LYP exchange-correlation energy functional. Polarizable continuum model of solvation was used to include solvent effects. The dielectric constant of the solvent was used while calculation of the energy levels. Molecules were first geometrically optimized by DFT calculations followed by energy calculations over the optimized structures. Optimized structure of (TPDC-DB)<sub>1</sub> is shown in Fig. S18 and the energy values are given in Table S3.

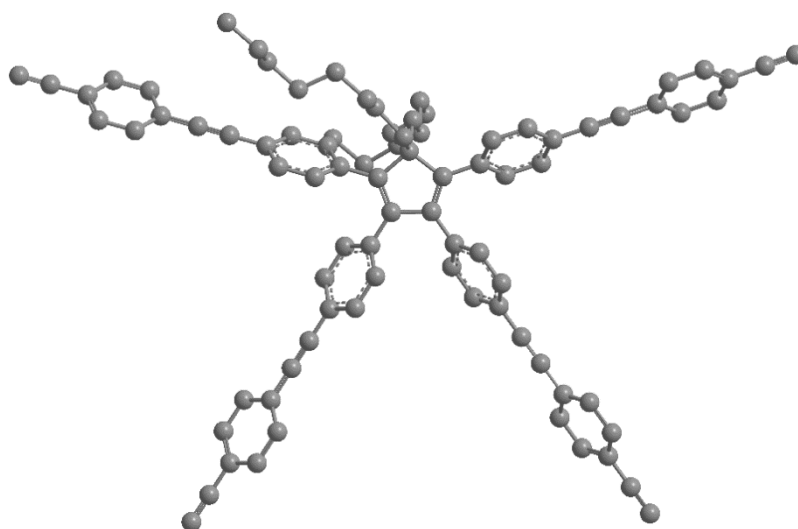


**Fig. S18.** Optimized structure of (TPDC-DB)<sub>1</sub>; all H atoms are omitted for clarity.

**Table S3.** Energy levels of different analytes and (TPDC-DB)<sub>1</sub> computed using DFT B3LYP/6-31G(d) with polarizable continuum model (PCM) of solvation.

Analyte	HOMO (eV)	LUMO (eV)
(TPDC-DB) <sub>1</sub>	-5.38	-2.01
Picric acid	-7.87	-3.53
2,4-dinitroaniline	-6.63	-2.74
<i>o</i> -nitrophenol	-6.68	-2.29
2,6-dichloro-4-nitroaniline	-6.42	-2.49
<i>p</i> -nitroaniline	-6.09	-2.17
<i>m</i> -nitroaniline	-6.01	-2.46
<i>o</i> -nitroaniline	-6.01	-2.32

## V. Electron paramagnetic resonance (EPR) spectroscopy

THF solution of TPDC-DB in presence of PNA was deoxygenated by purging with Ar. EPR spectra were recorded without and with photoexcitation with a free standing UV lamp at 365 nm (Fig. S19). The absence of any detectable signal ruled out the presence of cationic or anionic radical species. This corroborates the argument that PET is unlikely to govern the observed quenching trend.

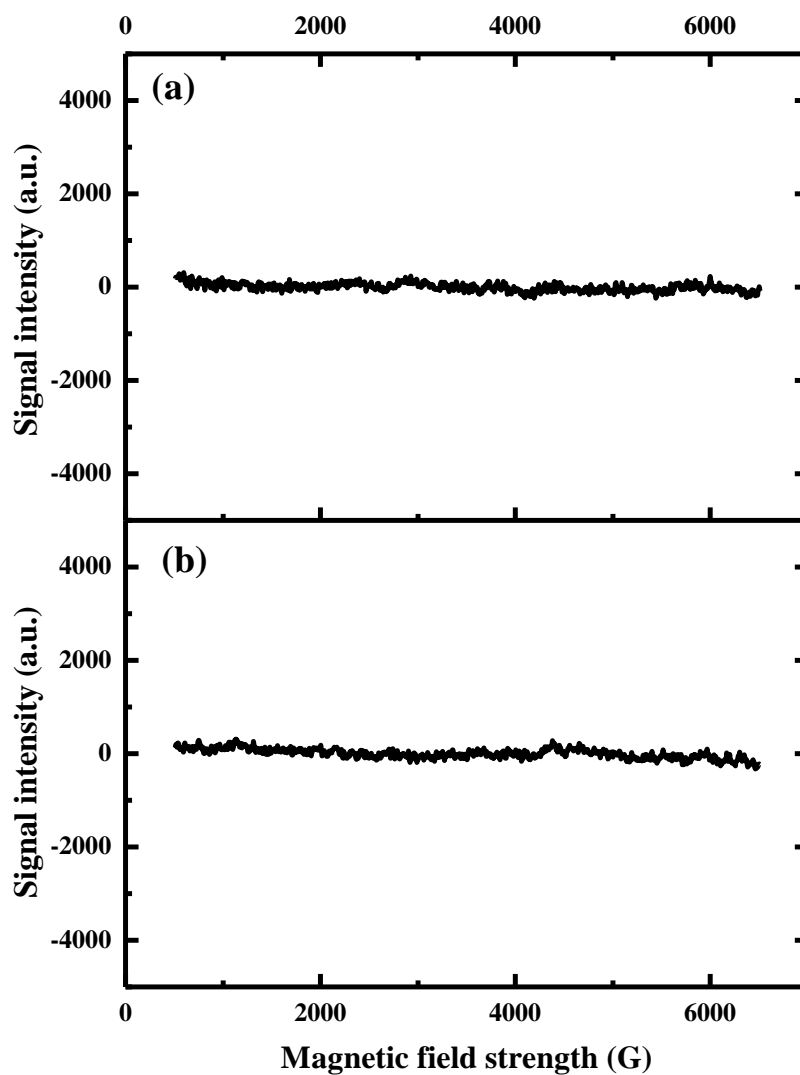


**Fig. S19.** EPR spectra of a mixture of TPDC-DB and PNA (a) under photoexcitation and (b) without photoexcitation.

## VI. Fitting curves for Stern-Volmer plots

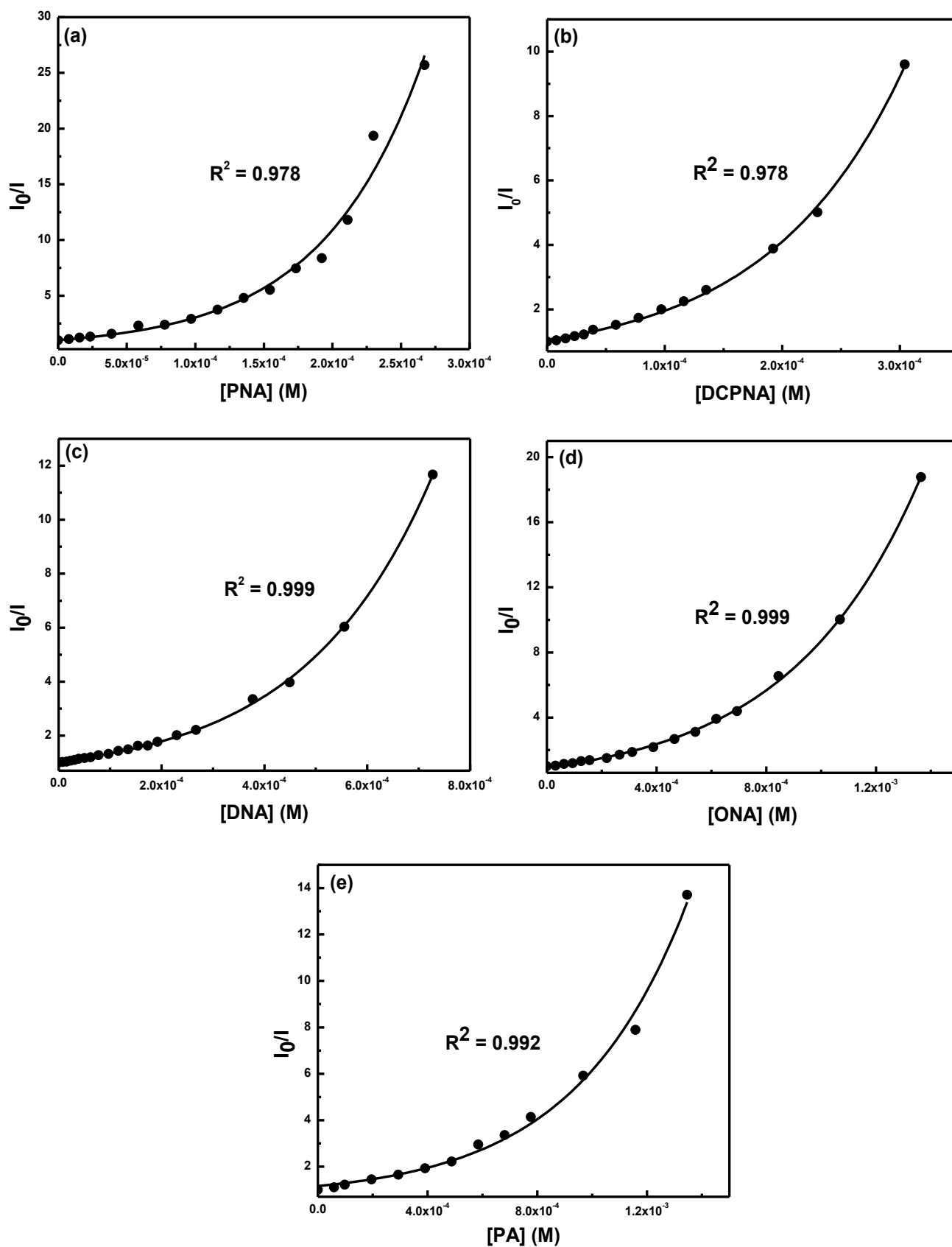


**Fig. S20.** Fitting curves for the Stern-Volmer plots of (a) PNA, (b) DCPNA, (c) DNA, (d) ONA and (e) PA.

## VII. Interactions of PNA and PA with TPDC-DB

In order to probe the interactions of nitroanilines and nitrophenols with TPDC-DB polymer, PNA, PA and first generation structure of the polymer (TPDC-DB)<sub>1</sub> were chosen as model systems. Molecular geometries of PNA, PA and (TPDC-DB)<sub>1</sub> were optimized using DFT under Gaussian 9.0 program package. Blend module in Materials Studio 6.1 was used to evaluate the nearest neighbour packing of PNA and PA with (TPDC-DB)<sub>1</sub>. Modified Flory-Huggins model and COMPASS force field were used to find the most stable cluster.<sup>3</sup> The obtained clusters were further optimized using DMol3 module with local-density approximation (LDA), VWN functional and DND basis set.<sup>4</sup> Different possible interactions (short contacts) of PNA and PA with (TPDC-DB)<sub>1</sub> are shown in the Fig. S21 and S22 respectively. Owing to the presence of two amino hydrogens, PNA shows more number of short contacts with  $\pi$ -conjugated framework (N-H $\cdots\pi$ , C-H $\cdots\pi$  etc.) demonstrating stronger interactions compared to that of PA.

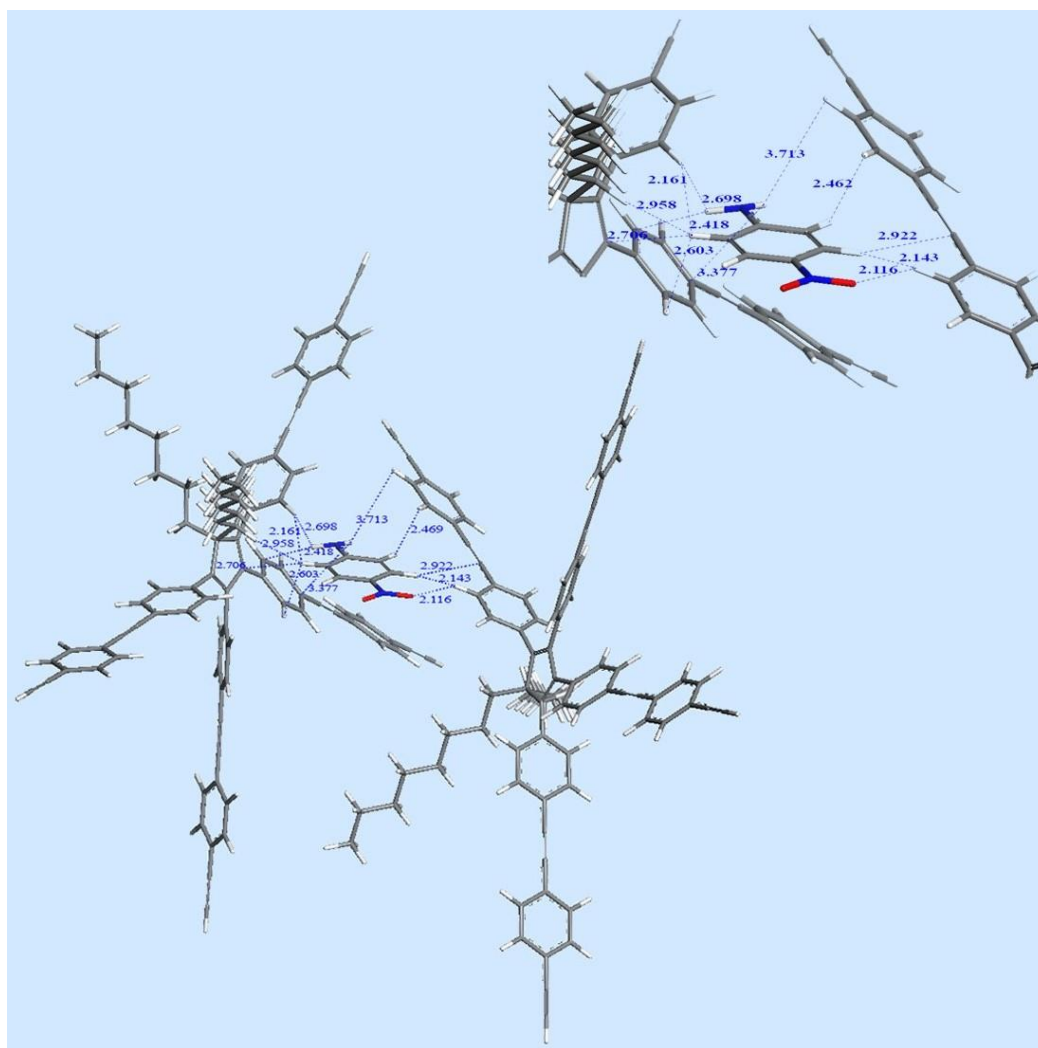


**Fig. S21.** Cluster depicting nearest neighbour packing of PNA with (TPDC-DB)<sub>1</sub>, short contacts are shown and distances are given in Angstrom; top right: magnified view.

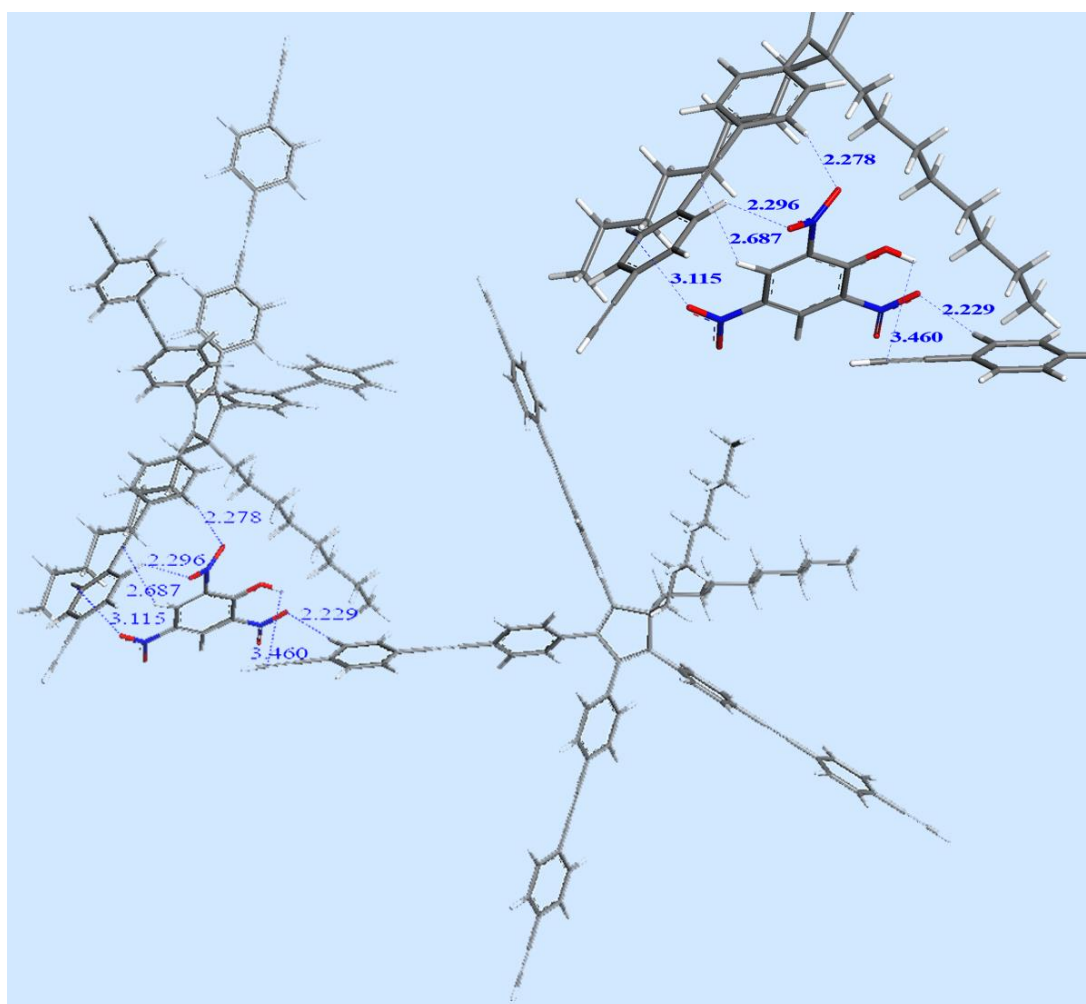


**Fig. S22.** Cluster depicting nearest neighbour packing of PA with (TPDC-DB)<sub>1</sub>, short contacts are shown and distances are given in Angstrom; top right: magnified view.

### VIII. Limit of detection (LOD)

(a) **Solution:** LOD was calculated by plotting fluorescence intensity of THF solution of TPDC-DB versus quencher concentration. The linear region of the resulting curve was fitted into a straight line (Fig. S23) and LOD was calculated according to the following equation (1)

$$LOD = 3\sigma/K$$

(1) where  $K$  = slope of the graph and  $\sigma$  = standard deviation of the intercept.<sup>5</sup>

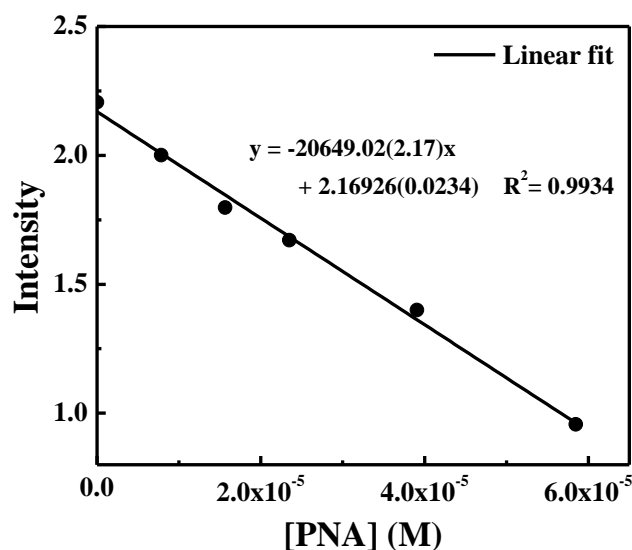


**Fig. S23.** Fluorescence intensity of TPDC-DB at  $\lambda_{em} = 468$  nm in THF solution as a function of PNA concentration and its linear fit, values in parentheses indicate the standard deviations in slope and intercept.

Therefore,

$$LOD = 3 \times 0.0234 / 20649.02 = 2.9 \times 10^{-6} M \approx 3 \mu M$$

$$LOD (ppb) = \frac{Wt\ of\ PNA}{Wt\ of\ solution} \times 10^9 = 455\ ppb$$

Similarly, LODs for DCPNA, DNA and ONA were obtained as  $4 \mu M$  (941 ppb),  $4.5 \mu M$  (936 ppb) and  $15 \mu M$  (2.35 ppm) respectively.

**(b) Contact mode:** For contact mode detection of *p*-nitroaniline, the detection limit was obtained by estimating the least amount of analyte per unit area of the spot.

$$\text{Detection limit} = \frac{\text{Minimum amt. of analyte}}{\text{Spot area}}$$

Therefore,

$$\text{Detection limit} = \frac{V \times C \times M}{A} = \frac{10^{-5} \times 10^{-6} \times 138.12}{0.8} = 1.77 \text{ ng.cm}^{-2} \approx 1.8 \text{ ng.cm}^{-2}$$

where, V, C and M are respectively the volume, concentration and molecular weight of the analyte added and A is the spot area.

### IX. Detection of PNA in presence of competing analytes

In order to study the quenching of TPDC-DB by PNA in presence of various interfering agents, emission intensity of a THF solution of TPDC-DB in presence of 0.1 M, 10  $\mu$ L of other competing analyte was measured. As shown in Fig. S24, the emission of TPDC-DB was barely quenched upon addition of various aliphatic amines, nitrobenzaldehydes, nitrotoluenes and other common compounds such as acrylamide, aniline, phenol, benzoquinone, mesitylene etc. When same concentration and volume of PNA was added to that solution, fluorescence was instantaneously quenched.

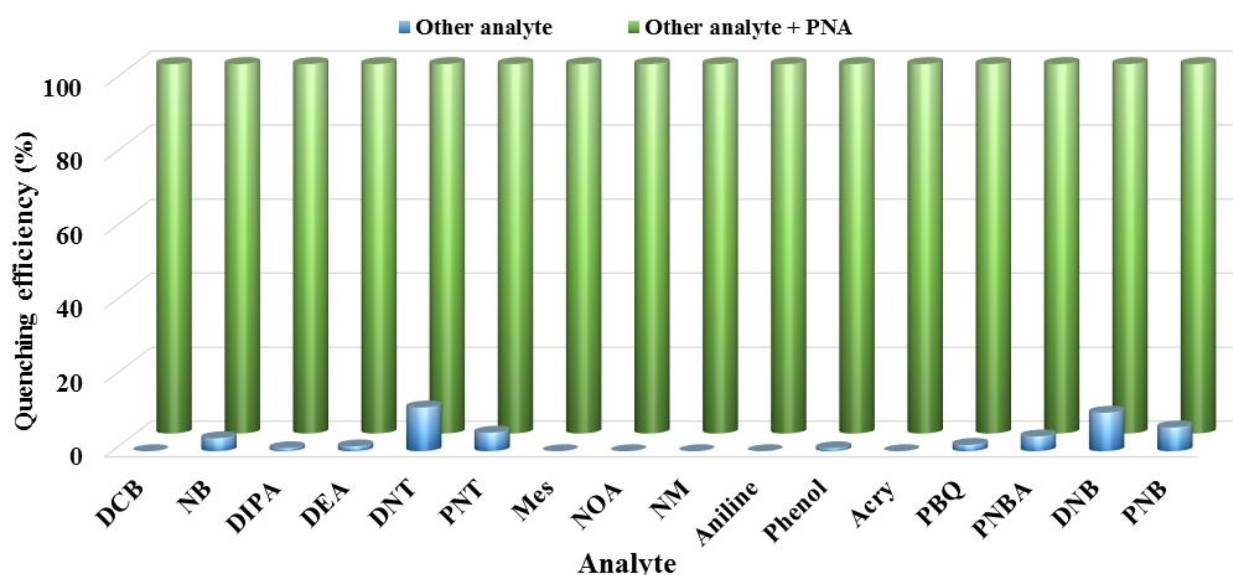


**Fig. S24.** Quenching efficiency (QE, in %) of a THF solution of TPDC-DB after addition of 0.1 M, 10  $\mu$ L of various competing analytes (blue) and that after addition of 0.1 M, 10  $\mu$ L PNA (green) to the same solution.

## X. Solid-state contact mode detection

THF solution of TPDC-DB ( $1 \text{ mg mL}^{-1}$ ) was drop casted on non-fluorescent TLC plates. Fluorescence spectra were recorded using front face geometry before and after the addition of various concentrations of aqueous solutions of PNA (Fig. S25).

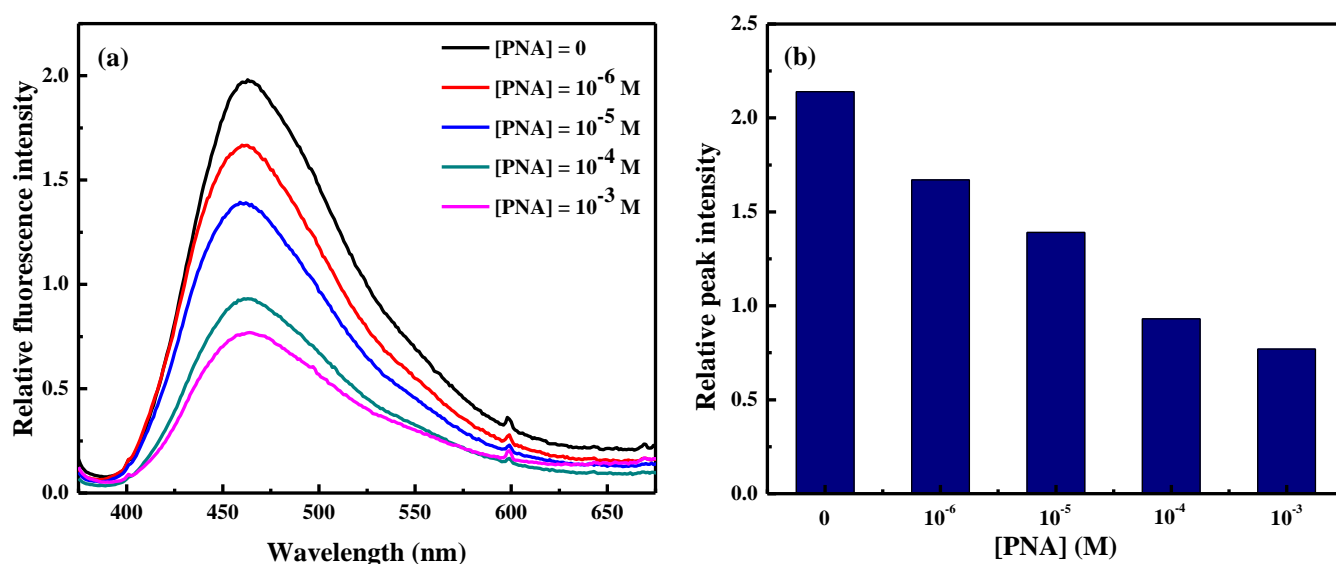


**Fig. S25.** (a) Solid-state fluorescence spectra ( $\lambda_{\text{ex}} = 365 \text{ nm}$ ) of TPDC-DB coated TLC plates with increasing concentration of PNA. (b) Relative change in the fluorescence intensity of TPDC-DB coated TLC plate against different concentrations of PNA.

## XI. Comparison of TPDC-DB with reported nitroaniline sensors

**Table S4.** A comparative account of nitroaniline detection by fluorescent materials.\*

Sr. No.	System	Nitroanilines/ nitroaromatics studied	Quenching constant ( $M^{-1}$ )	Sensitivity	Contact mode detection	Reference No.
1	<i>Present Manuscript</i>	<i>PNA, DCPNA, DNA, ONA, MNA</i>	$1.7 \times 10^4$ (PNA)	<i>455 ppb (PNA)</i>	<i>1.8 ng/cm<sup>2</sup> (PNA)</i>	-
2	Nitrogen-doped carbon dots	PNA, ONA, MNA, DNP, PNP, PNBA, MNBA	$1.25 \times 10^4$ (PNA)	$1 \times 10^{-7}$ M		6
3	Zn MOF	DNP, PNA, PNP, PNT, NB	-	4 ppm (PNA)	-	7
4	Zn MOF	NB, PNT, ONA, MNA, PNA p-chloronitrobenzene,	$5.99 \times 10^4$ (PNA)	-	-	8
5	Zn MOF, Cd MOF	PNA, aniline, p-toluidine, triethylamine	-	-	-	9
6	Zn MOF, Cd MOF	PNA, PNT, MNT, NB	$6.6 \times 10^3$ (PNA)	-	-	10
7	Phenanthro[4,5-fgh]- pyrido[2,3-b]quinoxaline	DNA, PNA, PNP, PA, DNP, ONA, MNA,	$2.94 \times 10^5$ (DNA), $1.07 \times 10^5$ (PNA)	0.05 ppm (DNA), 0.03 ppm (PNA)	9.1 ng (DNA) 13.8 ng (PNA)	11
8	Tetrazoleophenoxy polymer	2,4,6-trinitrobenzenesulfonic acid, NB, PNA 1-chloro-2,4-dinitrobenzene, 1-chloro-2-nitrobenzene	-	0.194 ppm (NB)	-	12
9	Naphthalimide-based fluorescent gelator	Aliphatic and aromatic amines including PNA	$6.29 \times 10^4$ (propyl amine)	$1.30 \times 10^{-7}$ M (propyl amine)	-	13
10	Perylenediimide based dye	PNA, ONA, MNA, PA, DNT, TNT, PNBA, PNP, NB	-	1 $\mu$ M	-	14
11	[Cu <sub>2</sub> (HTyr-N-Dan) <sub>4</sub> (H <sub>2</sub> O) <sub>2</sub> ].2H <sub>2</sub> O	PNA, ONA, DNA, PNP, ONP, NM	-	-	-	15
12	Calix[4]arene	PNA, ONA, MNA, NB, DNT, PNT etc.	$2.06 \times 10^4$ (PNA)	-	-	16
13	Pyrene and 1- methylpyrene	PNA, ONA, MNA, 4-methyl-3-nitroaniline, 2-methyl-4-nitroaniline, 4-methyl-3,5-dinitroaniline	$1.7 \times 10^4$ (PNA)	-	-	17
14	Carboxymethyl- $\beta$ - cyclodextrin-capped ZnO/ZnS/MgO Nanocomposites	PNA	-	$6.38 \times 10^{-7}$ mol L <sup>-1</sup>	-	18
15	UV-photolysis of 2-phenylbenz- imidazole-5-sulfonate	PNA, PNP, ONP, MNP	-	0.2 $\mu$ M	-	19

\*No report on detailed investigation of nitroaniline sensing by fluorescent porous organic polymers.

## XII. References

1. C. Wurth, M. Grabolle, J. Pauli, M. Spieles, U.R. Genger, *Nature Protocol*. 2013, **8**, 1535.
2. K. Rurak, M. Spieles, *Anal. Chem.*, 2011, **83**, 1232.
3. (a) K. S. Schweizer, J. G. Curro, *J. Chem. Phys.* 1989, **91**, 5059; (b) P. J. Flory, *Principles of Polymer Chemistry*, Cornell University Press, Ithaca, 1953.
4. V. A. Basiuk, Henao-Holguín, L. Verónica, *J. Comput. Theor. Nanos.* 2013, **5**, 1266.
5. S. Hussain, A. Malik, M. Afroz and P. K. Iyer, *Chem. Commun.* 2015, **51**, 7207.
6. H. Yuan, D. Li, Y. Liu, Xu and C. Xiong, *Analyst* 2015, **140**, 1428.
7. X. Wan, F. Jiang, C. Liu, K. Zhou, L. Chen, Y. Gai, Y. Yang and M. Hong, *J. Mater. Chem. A* 2015, **3**, 22369.
8. Z. Yu, F. Wang, X. Lin, C. Wang, Y. Fu, X. Wang, Y. Zhao and G. Li, *J. Solid State Chem.* 2015, **232**, 96.
9. F. Wang, C. Dong, C. Wang, Z. Yu, S. Guo, Z. Wang, Y. Zhao and G. Li, *New J. Chem.* 2015, **39**, 4437.
10. F. Wang, C. Wang, Z. Yu, Q. He, X. Li, C. Shang and Y. Zhao, *RSC Adv.* 2015, **5**, 70086.
11. P. Singla, P. Kaur and K. Singh, *Tetrahedron Lett.* 2015, **56**, 2311.
12. Y. Li, W. Zhang, Z. Sun, T. Sun, Z. Xie, Y. Huang and X. Jing, *Eur. Polym. J.* 2015, **63**, 149.
13. X. Pang, X. Yu, H. Lan, X. Ge, Y. Li, X. Zhen and T. Yi, *ACS Appl. Mater. Interfaces* 2015, **7**, 13569.
14. P. S. Hariharan, J. Pitchaimani, V. Madhu and S. P. Anthony, *J Fluoresc.* 2015, DOI 10.1007/s10895-015-1725-8.
15. N. Kumar, S. Khullar and S. K. Mandal, *RSC Adv.*, 2014, **4**, 47249.
16. J. Zhan, X. Zhu, F. Fang, F. Miao, D. Tian and H. Li, *Tetrahedron* 2012, **68**, 5579.
17. C. E. Agudelo-Morales, O. F. Silva, R. E. Galian and J. Pérez-Prieto, *ChemPhysChem* 2012, **13**, 4195.
18. Q. Gao, F. Liu, Y. Jiang, H. Dai, T. Fu and X. Kou, *Anal. Sci.* 2011, **27**, 851.
19. W. Zhang, C. R. Wilson and N. D. Danielson, *Talanta* 2008, **74**, 1400.